



**Original Research Article**

## **From Waste to Resources: Securing Incinerator Bottom Ash for Environmental Protection and Valorization**

Kouakou Benoit Kouame<sup>\*1</sup>, Koffi René Dongo<sup>1</sup>, Bi Gouesse Henri Briton<sup>1</sup>

<sup>1</sup>Laboratory of Industrial Processes for Synthesis, Environment, and New Energies (LAPISEN), Félix Houphouët-Boigny National Polytechnic Institute, P.O. Box 1093, Yamoussoukro, Côte d'Ivoire  
e-mail: [benoitk322@gmail.com](mailto:benoitk322@gmail.com)

Cite as: Kouame, K. B., Dongo, K. R., Briton, B. G. H., From Waste to Resources: Securing Incinerator Bottom Ash for Environmental Protection and Valorization, *J.sustain. dev. energy water environ. syst.*, 14(4), 1140754, 2026, DOI: <https://doi.org/10.13044/j.sdewes.d14.0754>

### **ABSTRACT**

Industrial incineration is widely used to treat potentially toxic waste, but the resulting bottom ash poses environmental and economic challenges. This study was motivated by the need to assess the potential reuse of bottom ash in sustainable applications. The working hypothesis was that quenching could influence ash homogeneity, trace metal distribution, and valorization potential. Bottom ash samples were analyzed for chemical composition, trace metal content, organic carbon, particle size, density, and mineralogical structure. Results show that the ash is mainly composed of iron, aluminum, silicon, and calcium oxides, with moderate organic content. Quenched bottom ash exhibited a more uniform particle size distribution, reduced variability in several trace metal concentration, and higher particle density compared with dry bottom ash. Statistical analysis showed reduced variability of chromium, nickel, cadmium, lead, and zinc after quenching. However, results should be interpreted cautiously due to the limited sample size and ash heterogeneity. Mineralogical analysis revealed ceramic fragments, glass phases, ferrous materials, and residual carbonaceous fractions. Quenching improved material homogeneity and indicates potential for reuse in construction applications. However, no leaching tests were performed; thus, environmental stability and mobility remain unconfirmed.

### **KEYWORDS**

Industrial waste, Bottom ash, Quenching, Trace metals, Physicochemical properties, Mineralogical characterization, Reuse potential.

### **INTRODUCTION**

Over the past few decades, waste management has shifted towards circular and sustainable strategies aimed at reducing landfilling and promoting resource recovery from waste. Within this framework, municipal solid waste incineration bottom ash (MSWI BA) has emerged as a promising secondary resource for construction and environmental applications. Nasrudin et al. [1] reviewed the incorporation of industrial by-products into concrete and highlighted the environmental benefits associated with reducing the consumption of virgin raw materials. Hamada et al. [2] reported that coal bottom ash can successfully replace natural fine aggregates while maintaining satisfactory mechanical and durability properties. Chen et al.[3] demonstrated that MSWI bottom ash can be incorporated into high-performance cementitious composites, whereas Jin et al.[4] showed that cold-bonded granulation improves the engineering performance and recycling potential of bottom ash aggregates. Similarly, Xiao et al.[5] emphasized the growing importance of recycled aggregates in sustainable construction

<sup>\*</sup> Corresponding author

practices. The increasing interest in bottom ash valorization is largely related to its significant mineral content and potential use as a substitute for natural resources. Bayuseno and Schmahl [6] reported that bottom ash contains a complex assemblage of silicates, oxides, glassy phases, and metallic particles resulting from high-temperature incineration processes. Minane and Vinai [7] further highlighted that the composition of bottom ash varies considerably according to waste characteristics, combustion conditions, and cooling methods. Huang *et al.* [8] demonstrated that these variations strongly influence both mechanical performance and heavy-metal release when bottom ash is used in road embankments. Šyc *et al.* [9] identified the heterogeneous distribution of metals as one of the main challenges affecting the recycling of incineration residues. Despite its potential for reuse, environmental concerns remain a major obstacle to the large-scale utilization of bottom ash. Van der Sloot *et al.* [10] established that the environmental acceptability of waste-derived materials depends primarily on their leaching behavior. Meima and Comans [11] demonstrated that weathering reactions control the evolution of mineral phases and contaminant release over time. More recently, Hammoud *et al.* [12] successfully modeled the geochemical mechanisms governing trace-metal leaching from MSWI bottom ash. He and Kasina [13] further showed that several heavy metals remain potentially mobile in untreated ashes, depending on their chemical speciation. Similar observations were reported by Izquierdo and Querol [14] for coal combustion residues. Simon and Scholz [15] confirmed that long-term leaching behavior remains one of the key environmental issues limiting bottom ash reuse and highlighted the influence of mineralogical evolution on contaminant release. Several studies have therefore investigated treatment processes aimed at improving the environmental stability of bottom ash. Dijkstra *et al.* [16] demonstrated that accelerated aging significantly modifies the mechanisms controlling copper and molybdenum release. Kubota *et al.* [17] reported that combined aging and washing treatments effectively reduce long-term leaching potential. Lombardi and Carnevale [18] showed that on-site treatment can enhance the suitability of bottom ash for recycling applications. Glause *et al.* [19] through a ten-year monitoring program, revealed that total organic carbon (TOC) progressively decreases during aging while leaching behavior evolves significantly. More recently, Xiao *et al.* [20] observed substantial modifications in pore structure, surface area and mineralogical characteristics during seasoning processes, confirming that aging strongly affects bottom ash properties.

The influence of cooling conditions has received increasing attention because of its direct impact on ash formation and subsequent behavior. Most waste-to-energy plants discharge bottom ash through water quenching immediately after combustion, generating rapid physicochemical transformations. A recent review highlighted that wet-discharge bottom ash exhibits high heterogeneity, unstable mineral phases and elevated contaminant mobility compared with aged materials. Inkaew *et al.* [21] demonstrated that water quenching induces the formation of calcium-silicate-hydrate phases, Friedel's salt, hydrocalumite and portlandite, significantly modifying ash morphology and mineralogy. The authors further showed that quenching products form preferentially around fine particles, contributing to ash heterogeneity and influencing subsequent weathering processes. These findings suggest that cooling conditions may play a critical role in determining the environmental and engineering performance of bottom ash. In parallel, alternative valorization pathways have emerged. Samaka *et al.* [22] demonstrated that furnace bottom ash can be used as a low-cost adsorbent for phosphate removal from water. Lin *et al.* [23] developed high-performance adsorbents derived from MSWI bottom ash, while Zhao *et al.* [24] reported promising heavy-metal removal efficiencies and highlighted the role of ash-derived materials in circular economy strategies. Although considerable progress has been achieved regarding municipal bottom ash, industrial bottom ash remains comparatively under-investigated, particularly in developing countries and tropical environments. Furthermore, most previous studies focused separately on environmental, mineralogical, or engineering aspects. Integrated investigations combining

physicochemical composition, mineralogical characteristics, total organic carbon, trace-metal distribution and geotechnical properties remain scarce. Moreover, the specific effects of wet quenching on ash heterogeneity, mineral transformations, TOC evolution and metal distribution are still insufficiently documented. Therefore, the present study investigates the influence of wet quenching on the physicochemical, mineralogical and geotechnical characteristics of industrial bottom ash. The working hypothesis is that wet quenching induces physicochemical transformations that may affect ash homogeneity, trace metal distribution, and reuse potential. To test this hypothesis, major oxides, trace metals, total organic carbon, particle size distribution, density, and mineralogical composition were systematically analyzed. The study aims to provide a comprehensive characterization of industrial bottom ash while discussing the implications of quenching for future management and potential reuse applications., combined with statistical analysis to assess variability and stability.

## MATERIALS AND METHODS

Industrial incineration bottom ash was characterized for chemical composition, trace metals, total organic carbon, particle size, density, and mineralogical fractions. Thermal and chemical treatments were applied to assess stabilization effects. Statistical analyses evaluated variability, stability, and valorization potential.

### Materials

The study focused on two industrial bottom ash types generated from comparable industrial waste streams under different ash extraction and cooling conditions:

- Dry bottom ash (ATI HP1000)
- Quenched bottom ash (ATI HP1250)

The principal difference between the two materials was the ash cooling and collection process. ATI HP1000 bottom ash was collected under dry conditions after air cooling, whereas ATI HP1250 bottom ash underwent wet quenching immediately after incineration.

A total of 14 samples were collected (7 samples per ash type). The sampling strategy was designed to account for the intrinsic heterogeneity of bottom ash materials following representative waste sampling principles described in EN 14899. For physicochemical analyses, five individual samples of approximately 400 g were collected for each ash type in order to evaluate parameter variability. For mineralogical analyses, one composite sample of 1 kg per ash type was prepared by homogenizing representative subsamples. For geotechnical characterization, a composite sample of 50 kg per ash type was prepared.

Sampling was performed at representative ash discharge zones after stabilization of operational conditions while avoiding external contamination. This sampling methodology, combining individual and composite samples, ensures both the analysis of physico-chemical variability and a comprehensive representation of the mineralogical and geotechnical properties of the bottom ash studied. Figure 1 shows the two types of bottom ash studied.

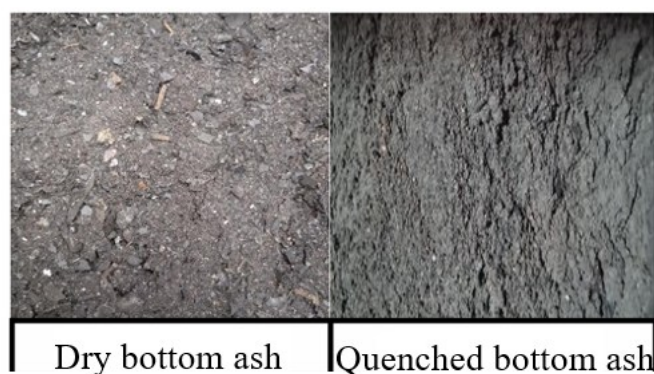


Figure 1. Photograph of the studied bottom ash

## Methods

This section describes the experimental procedure and the analytical methods used to investigate the physicochemical, mineralogical, geotechnical properties of the industrial bottom ash and Statistical analysis.

### Experimental procedure

All bottom ash samples were air-dried at room temperature for 72 h and manually homogenized. Coarse metallic debris and oversized particles were removed prior to analysis. The samples were then crushed using an agate mortar and sieved to obtain particle sizes below 100  $\mu\text{m}$ . The prepared powders were stored in airtight polyethylene containers until analysis.

Major oxides were determined by X-ray fluorescence (XRF) using pressed powder pellets prepared from finely ground dried samples. Approximately 5 g of powder were mixed with a binder and pressed into pellets under hydraulic pressure. The granulometry of the analyzed powders was maintained below 100  $\mu\text{m}$  to improve analytical homogeneity and measurement reproducibility.

XRF calibration was performed using certified reference materials (CRMs), including National Institute of Standards and Technology standards (NIST SRM 2711a) and geological reference materials such as BCR-2. Mineralogical phases were identified by X-ray diffraction (XRD) using powdered samples scanned over an angular range of  $5\text{--}70^\circ 2\theta$ .

Instrument performance and analytical precision were checked regularly using calibration standards and duplicate analyses. Mineralogical phases were identified by X-ray diffraction (XRD) using powdered samples scanned over an angular range of  $5\text{--}70^\circ 2\theta$ . The analyses were performed under controlled operating conditions, including appropriate scanning speed, step size, and tube voltage settings to ensure reliable phase identification.

The method for determining the parameters analyzed in the slag and the objectives pursued are recorded in Table 1.

Table 1. Analytical parameters, determination methods, and objectives.

Category	Analyzed parameter	Analytical method	Objective of the analysis
Major chemical composition	Major oxides	X-ray fluorescence (XRF)	To determine the overall chemical composition and assess the valorization potential of incineration bottom ash
Metallic pollution	Trace metal elements	ICP-OES / ICP-MS after acid digestion	To evaluate contamination levels and associated environmental risks
Thermal characterization	Loss on ignition (LOI)	Thermogravimetric analysis (calcination in a high-temperature furnace at $\sim 950^\circ\text{C}$ )	To estimate the volatile fraction and residual combustible compounds
Mineralogical characterization	Crystalline mineral phases	X-ray diffraction (XRD) on 40–50 g samples	To identify mineral phases and assess chemical stability
Residual organic matter	Total organic carbon (TOC)	TOC analyzer (thermal or chemical oxidation)	To quantify residual organic matter and assess environmental impact

### Geotechnical Parameters

The geotechnical characterization of bottom ash focused on particle size distribution, bulk density, and apparent density, as detailed in Table 2.

### Particle Size Analysis

The particle size distribution of the fine fraction (0.063–2 mm) was determined by dry sieving using a Retsch AS 200 vibrating sieves equipped with standardized sieves. The particle size analyses, carried out in triplicate on 400 g samples, allowed the calculation of the uniformity coefficient (CU, NF P 18-540) to assess particle size homogeneity, the curvature coefficient (Cc) to characterize the shape of the particle size distribution, and the fineness modulus (Mf, EN 12620) to evaluate the proportion of fine and coarse grains for potential use as aggregates in concrete.

#### Bulk density and apparent density

Bulk density ( $\rho$ ) was measured by helium pycnometry according to ISO 17892-3, allowing for the consideration of the open pores of the particles. The apparent density ( $\rho_{ap}$ ), corresponding to the mass of a given volume including intergranular voids, was determined in accordance with standard NF EN 1097-3. These analyses provide essential information on the particle size distribution, compaction, and porosity of bottom ash, which are key factors for their use in construction materials or their environmental behavior. The uniformity coefficient (UC) was calculated using Equation  $UC = \frac{D_{60}}{D_{10}}$  (1), the coefficient of curvature (Cc) was determined using Equation  $CC = \frac{D_{30}^2}{D_{60}D_{10}}$  (2), and the fineness modulus (FM) was computed according to Equation  $FM = \frac{1}{100} \sum \text{cumulative retained (0.16; 0.315; 0.63; ...; 5)}$  (3).

Table 2. Provides a summary of the methods and reference standards in force

Method / Equipment	Formula	Standard
Uniformity coefficient (UC) Calculation from the particle size distribution curve	$UC = \frac{D_{60}}{D_{10}}$ (1)	NF P 18-540
Coefficient of curvature (Cc) Calculation from the particle size distribution curve	$C_c = \frac{D_{30}^2}{D_{60}D_{10}}$ (2)	NF P 18-540
Fineness modulus (FM) Sum of cumulative percentages retained on sieves 0.16–5 mm	$F_M = \frac{1}{100} \sum \text{cumulative retained (0.16; 0.315; 0.63; ...; 5)}$ (3)	EN 12620
Particle size distribution Dry sieving using a vibratory sieve shaker (Retsch AS 200)	-	NF P 18-540
True particle density ( $\rho$ ) Helium pycnometry	-	ISO 17892-3
density ( $\rho_{ap}$ ) Weighing in a cylindrical container of known volume	-	NF EN 1097-3

### Statistical analysis

Descriptive statistics were calculated for all physicochemical parameters. Due to the limited sample size and the heterogeneous nature of bottom ash materials, statistical interpretations were performed cautiously.

The Shapiro–Wilk test was used only as an exploratory indicator of data distribution. However, because of the small sample size ( $n = 7$  per group), normality assumptions could not be considered conclusive.

Comparisons between dry bottom ash (ATI HP1000) and quenched bottom ash (ATI HP1250) were performed using the non-parametric Mann–Whitney U test. The objective of the analysis was to identify possible differences associated with ash cooling conditions rather than to establish definitive causal relationships. Statistical significance was considered at  $p < 0.05$ .

Individual values and boxplots were additionally presented to visualize variability and dispersion within each ash type.

## RESULTS AND DISCUSSION

For simplicity and improved readability throughout the manuscript, dry bottom ash samples are hereafter referred to as AT1, whereas quenched bottom ash samples are referred to as AT2.

### Chemical oxides

The chemical oxide contents of the slags and their comparison between the non-leached samples (AT1) and leached samples (AT2) are presented in Table 3 and visualized as comparative boxplots in Figure 2. Grouped boxplots of Major elements

Table 3. Chemical oxides contents of the slags

Chemical oxides	Average AT1 (%) + Standard deviation [ppm]	Average AT2 (%) + Standard deviation [ppm]
Fe <sub>2</sub> O <sub>3</sub>	21.80 ± 12.00	13.00 ± 11.60
MnO	0.13 ± 0.03	0.15 ± 0.07
TiO <sub>2</sub>	3.00 ± 5.50	2.30 ± 1.00
CaO	21.90 ± 12.20	28.00 ± 13.20
K <sub>2</sub> O	0.61 ± 0.18	0.51 ± 0.15
Al <sub>2</sub> O <sub>3</sub>	4.80 ± 0.60	6.70 ± 2.10
P <sub>2</sub> O <sub>5</sub>	0.33 ± 0.21	0.77 ± 0.45
SiO <sub>2</sub>	23.20 ± 3.00	23.10 ± 5.00
MgO	1.25 ± 0.25	1.08 ± 0.14
SO <sub>3</sub>	0.99 ± 0.35	0.84 ± 0.25
Na <sub>2</sub> O	< 0.2	0.19 ± 0.14

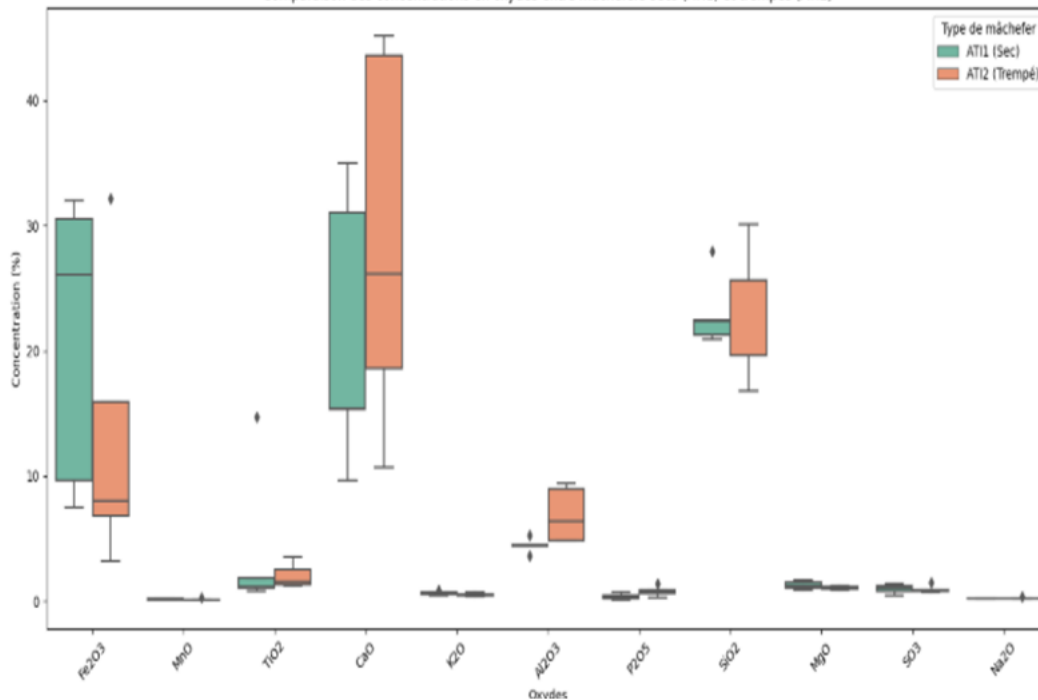


Figure 2. Grouped boxplots of Major elements

The analyzed slags are dominated by  $\text{Fe}_2\text{O}_3$ ,  $\text{CaO}$ ,  $\text{Al}_2\text{O}_3$ , and  $\text{SiO}_2$ , with proportions varying according to the samples, reflecting the heterogeneity of the incinerated waste [8].  $\text{SiO}_2$  and  $\text{Al}_2\text{O}_3$ , comparable to feldspars, provide potential for ceramic applications [25], while the high  $\text{CaO}$  in AT2 suggests suitability for soil amendment, improving pH and fertility [26].  $\text{Fe}_2\text{O}_3$ , more variable in AT1, contributes to the stability and corrosion resistance of the material [27].

The quenching (AT2) concentrates basic oxides ( $\text{CaO}$ ,  $\text{Al}_2\text{O}_3$ ,  $\text{P}_2\text{O}_5$ ) through crystallization and loss of soluble phases, while the oxides  $\text{SiO}_2$ ,  $\text{K}_2\text{O}$ ,  $\text{MgO}$ ,  $\text{SO}_3$  remain stable and  $\text{Na}_2\text{O}$  appears in traces. These changes indicate that quenching homogenizes the chemical composition and stabilizes the slags, optimizing their use in construction materials or as agricultural amendments, while improving the reproducibility of their physical properties.

### Metallic trace elements and the effect of quenching

The concentrations of metallic trace elements (MTEs) in non-quenched (AT1) and quenched (AT2) bottom ashes are summarized in Table 4, accompanied by comparative boxplots shown in Figure 3. Grouped boxplots of trace metal concentrations (Ba, Cr, Cu, Ni, Cd, Mo, Hg, As, Pb and Zn) in AT1 and AT2 samples. This representation allows visualization of differences in concentration, the dispersion of metals, and the stabilizing effect of quenching on MTEs, particularly for toxic metals at low concentrations such as Cd and Hg.

Table 4. Concentrations of metallic trace elements (MTEs) in non-quenched (AT1) and quenched (AT2) bottom ashes

MTEs	Average AT1 (ppm) $\pm$ SD	Average AT2 (ppm) $\pm$ SD	Detection limit (ppm)
Ba	1832.83 $\pm$ 452.66	2220.94 $\pm$ 1727.63	1
Cr	514.48 $\pm$ 232.77	265.05 $\pm$ 110.07	0.01
Cu	697.13 $\pm$ 894.61	2722.59 $\pm$ 3760.48	0.2
Ni	189.50 $\pm$ 134.87	162.69 $\pm$ 58.3	0.2
Cd	0.178 $\pm$ 0.036	0.076 $\pm$ 0.0134	0.01
Mo	41.24 $\pm$ 25.17	39.90 $\pm$ 21.15	0.4
Hg	0.034 $\pm$ 0.020	0.028 $\pm$ 0.004	0.1
As	39.18 $\pm$ 19.53	47.51 $\pm$ 29.14	0.2
Pb	781.35 $\pm$ 1439.02	181.42 $\pm$ 318.17	0.02

Zn	2212.84 ± 2258.31	1777.5 ± 1449.84	0.2
----	-------------------	------------------	-----

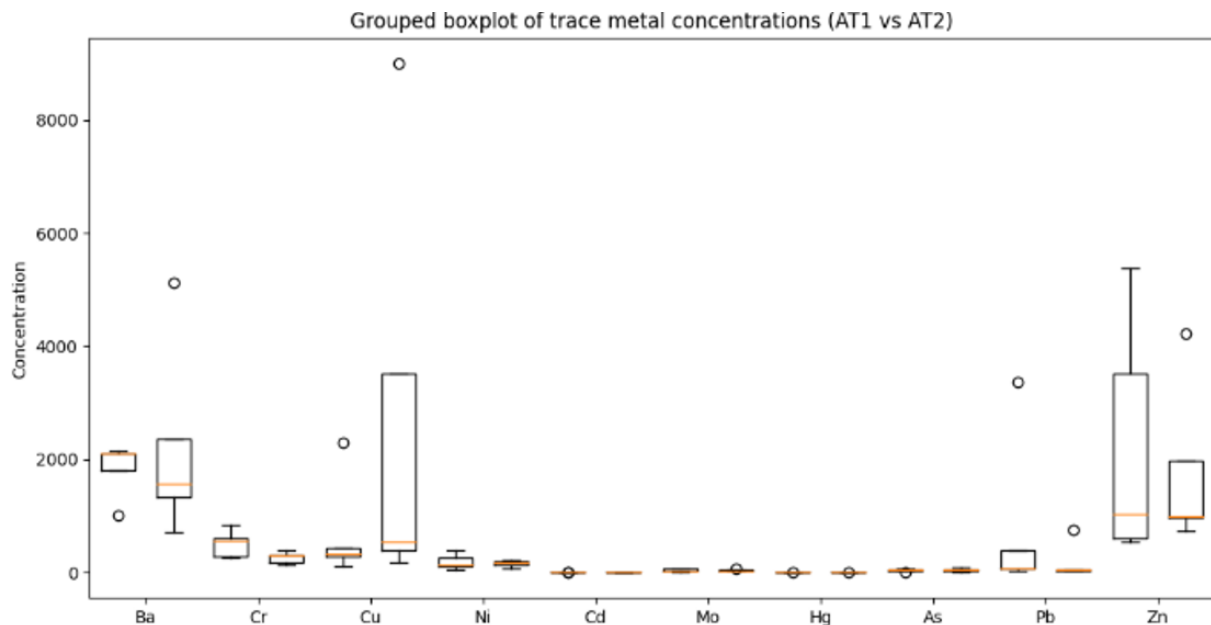


Figure 3. Grouped boxplots of trace metal concentrations (Ba, Cr, Cu, Ni, Cd, Mo, Hg, As, Pb and Zn) in AT1 and AT2 samples

The analysis of trace metals clear differences between dry bottom ash (AT1) and quenched bottom ash (AT2). Overall, AT1 exhibited higher median concentrations and wider dispersion for most elements (Ba, Cr, Cu, Ni, Pb and Zn), indicating a more heterogeneous matrix. Šy et al.[9] reported that the heterogeneous distribution of mineral and metallic phases is a characteristic feature of bottom ash and can result in significant variability in elemental composition. This observation agrees with the greater dispersion measured in AT1. This behavior is consistent with the findings of Cases and Thomas [28], who reported that untreated or freshly produced bottom ash generally shows strong spatial and chemical heterogeneity due to incomplete stabilization reactions at early stages. In contrast, AT2 showed reduced variability for several metals, particularly Cr, Ni, Pb, Zn and Cd. This trend may be related to physicochemical transformations induced by wet quenching, including dissolution of soluble phases, hydration reactions, carbonation and mineral aging. According to Meima and Comans [11], weathering processes progressively modify the mineralogical structure of bottom ash and contribute to improved chemical stabilization through carbation and formation of secondary minerals.

Copper remained relatively variable in both AT1 and AT2, which is also reported in the literature. Studies such as Song et al. [29] have shown that Cu often exhibits weaker stabilization during aging processes due to its association with organic matter or less reactive mineral phases. This explains the partial persistence of heterogeneity observed in this study.

Although Cd and Hg concentrations were low in both conditions, their environmental relevance remains high due to their toxicity and mobility potential. The reduction in variability observed in AT2 for Cd is in agreement with the work of Izquierdo and Querol[14], who reported that wet treatment and carbonation processes can reduce the mobility of certain trace metals by promoting their incorporation into stable mineral phases. Nevertheless, some divergences from the literature can be noted. While several studies report a strong reduction in overall metal concentrations after extended aging or leaching conditions, the present study focuses on total metal content rather than leachable fractions. This methodological difference

likely explains why the observed reductions are mainly expressed as variability changes rather than strong decreases in absolute concentrations.

AT1 showed higher variability and wider dispersion ranges for Cu, Pb, and Zn compared with AT2, indicating greater heterogeneity of the untreated material. In contrast, AT2 exhibited narrower distributions for Cd, Pb, and Zn, suggesting improved physicochemical homogeneity after wet quenching. The observed trends suggest that wet quenching contributes to bottom ash maturation and partial trace metal stabilization. Nevertheless, only total metal concentrations were measured in this study. No leaching tests were performed; therefore, conclusions regarding reductions in metal mobility or environmental risk should be interpreted cautiously. AT1 showed higher variability and wider dispersion ranges for Cu, Pb, and Zn compared with AT2, indicating greater heterogeneity of the untreated material. In contrast, AT2 exhibited narrower distributions for Cd, Pb, and Zn, suggesting improved physicochemical homogeneity after wet quenching. The observed trends suggest that wet quenching contributes to bottom ash maturation and partial trace metal stabilization. Nevertheless, only total metal concentrations were measured in this study. No leaching tests were performed; therefore, conclusions regarding reductions in metal mobility or environmental risk should be interpreted cautiously. As emphasized by Meima and Comans [11], total metal content alone is insufficient to assess environmental behavior, which mainly depends on metal speciation and leaching properties. Additional treatments may contribute to the stabilization of trace metals and improve the suitability of bottom ash for potential reuse applications. Maturation processes described in previous studies involve progressive physicochemical transformations of bottom ash. Dijkstra *et al.* [16] demonstrated that accelerated aging significantly modifies the mechanisms controlling trace-metal release. Kubota *et al.* [17] showed that aging and washing treatments promote the stabilization of reactive phases and reduce long-term leaching potential. Glauser *et al.* [19] further reported that long-term weathering is accompanied by changes in total organic carbon content and mineralogical composition. These processes involve oxidation of metallic particles, carbonation of lime-bearing phases and progressive mineral aging, which may reduce pH, influence trace-metal behavior and improve geotechnical stability. Similarly, the Tredi-ASH process has been reported to promote partial removal of certain metals, potentially contributing to the production of more stable residues [30]. In this context, wet quenching combined with maturation processes may contribute to partial trace metal stabilization and reduced variability of toxic elements such as Cd and Hg. These transformations could improve the potential use of bottom ash in construction materials such as bricks, pavers, or expanded clay, although additional leaching and environmental assessment studies would be required to confirm long-term safety and stability.

### **Statistical analysis of trace metal elements**

The comparative boxplot (Figure 4) shows that untreated slags (AT1) have higher median concentrations and wider interquartile ranges for most trace metals, reflecting high heterogeneity. Quenched slags (AT2) exhibit lower medians and reduced dispersion, particularly for Cr, Ni, Cd, Pb, and Zn, indicating improved metal stabilization. Only Cu, Hg, and Pb display an approximately normal distribution (Figure 4. Data distribution according to the Shapiro-Wilk test for dry bottom ash and Figure 5. Data distribution according to the Shapiro-Wilk test for wet bottom ash), while the other metals do not, justifying the use of the non-parametric Mann–Whitney U test. This analysis reveals statistically significant decreases ( $p < 0.05$ ) in the median concentrations and variability of Cr, Ni, Cd, Pb, and Zn after quenching.

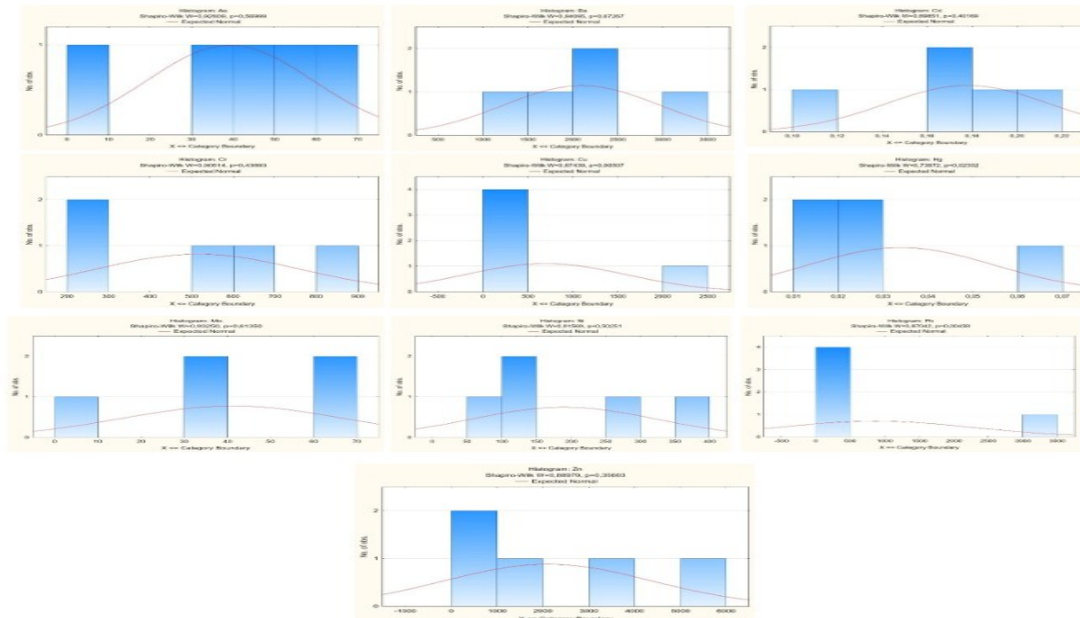


Figure 4. Data distribution according to the Shapiro-Wilk test for dry bottom ash

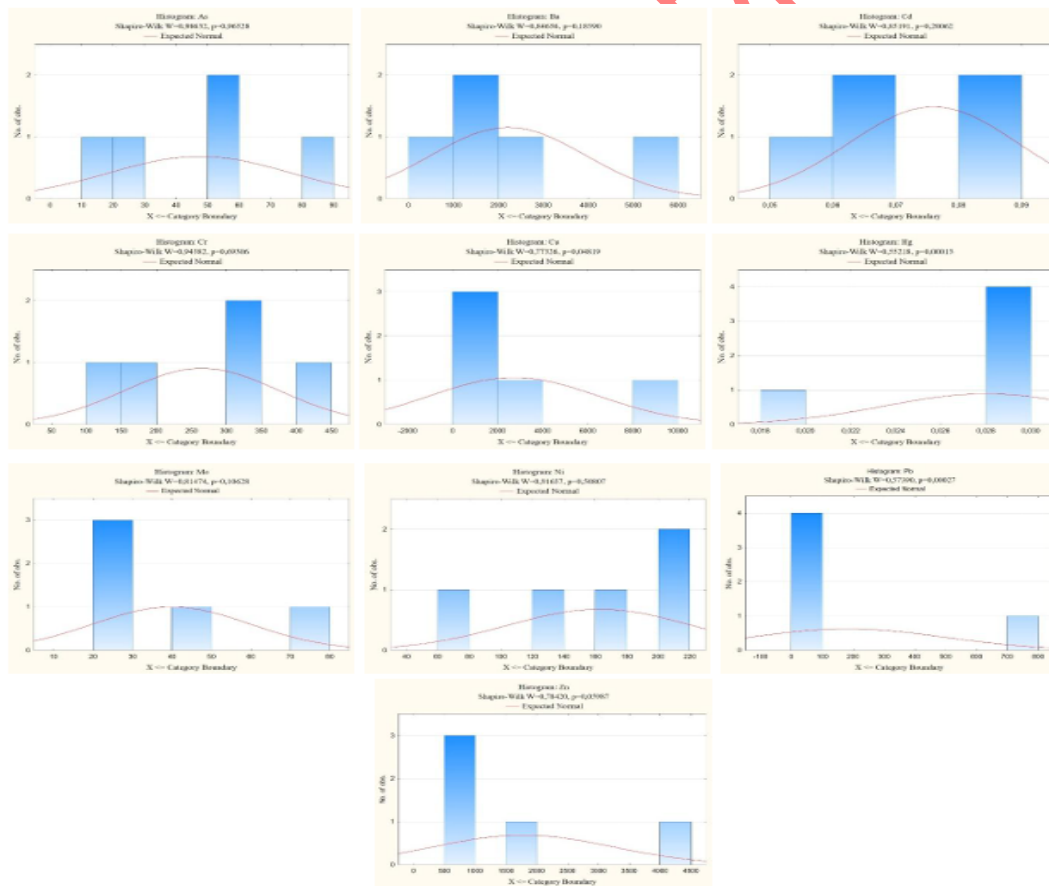


Figure 5. Data distribution according to the Shapiro-Wilk test for wet bottom ash

### Dry Matter Content

The measured material losses for all the slag samples range from 8.97% to 39.57% (Figure 6).

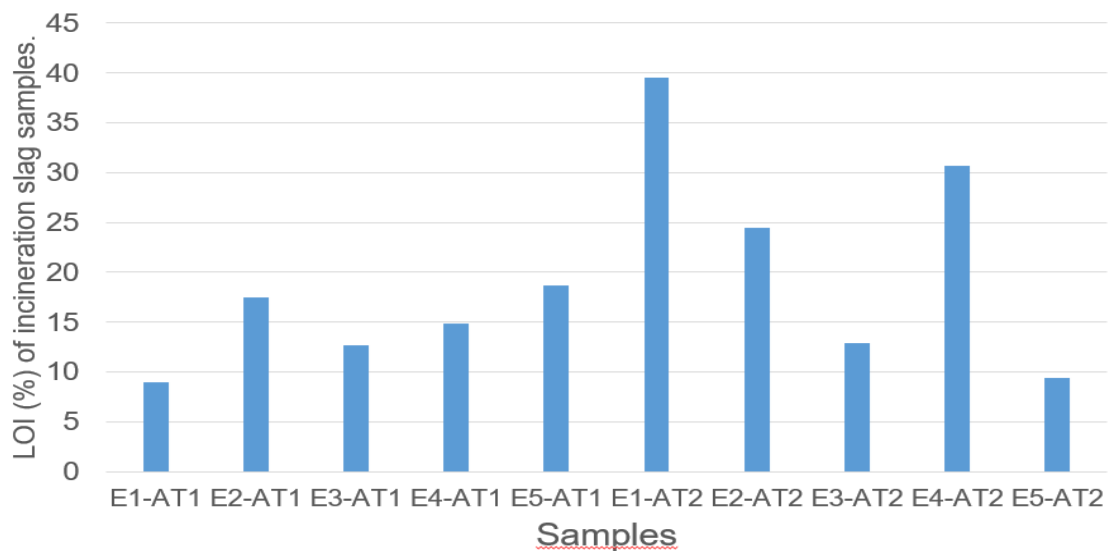


Figure 6. Percentage of mass loss by sample

For samples from the AT1 treatment (untreated slag), losses vary from 8.97% (E1-AT1) to 18.66% (E5-AT1), with relatively moderate variation. In contrast, samples from the AT2 treatment (soaked slag) show significantly higher and more variable losses, ranging from 9.36% (E5-AT2) to 39.57% (E1-AT2). In general, the values observed for AT2 are higher than those for AT1, except for samples E3 and E5, for which comparable or even lower losses are recorded after soaking.

Shapiro–Wilk tests (AT1:  $p = 0.80$ ; AT2:  $p = 0.76$ ) indicate that the material losses follow a non-normal distribution. The observed variations reflect the intrinsic heterogeneity of the incinerated waste, related to the diversity of incoming streams and their varying proportions. Soaked bottom ash (AT2) generally exhibits higher losses, attributable to the combined effect of soaking and thermal shock, which promotes the dissolution of soluble phases, the entrainment of fines, and the disintegration of the mineral matrix, as observed for E1-AT2 (39.57%) and E4-AT2 (30.63%). Conversely, the low losses measured for certain samples, notably E1-AT1 (8.97%) and E5-AT2 (9.36%), indicate a content of poorly leachable mineral phases. These results suggest that dry bottom ash is generally more favorable for valorization than soaked bottom ash.

### Total Organic Carbon

Figure 7 and Figure 8 show, respectively, the variation of TOC in the different samples analyzed and the comparison between the two types.

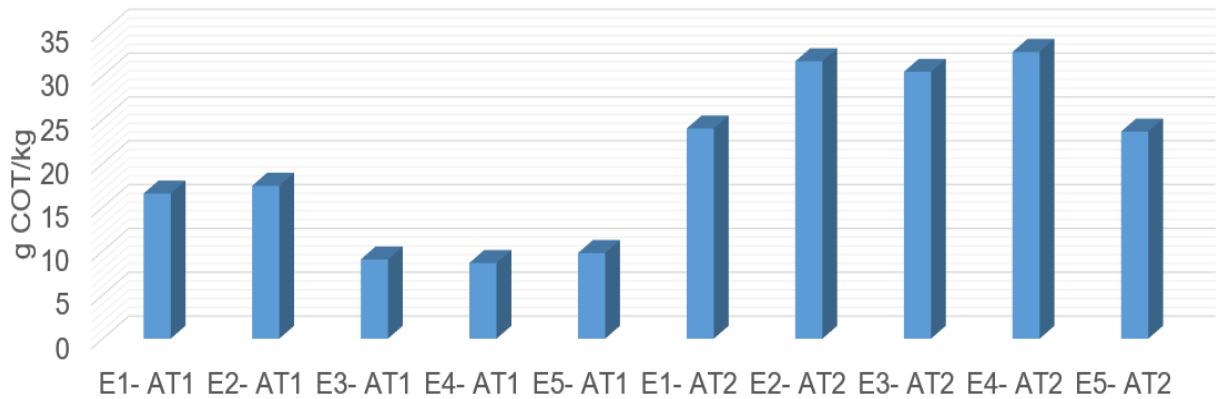


Figure 7. Variation of TOC in the different samples analyzed

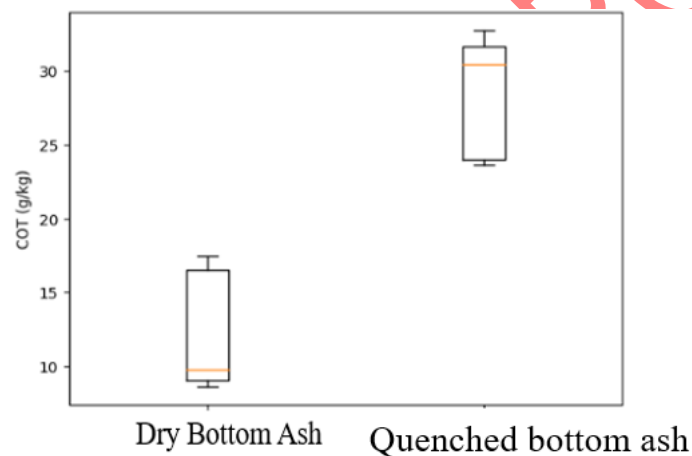


Figure 8. Comparison between the two types

AT1 shows TOC contents ranging from 8.6 to 17.5 g/kg, significantly lower than those of AT2, which range from 23.6 to 32.7 g/kg. The Mann–Whitney U test confirms a significant difference between AT1 and AT2 ( $p < 0.05$ ). Residual total organic carbon (TOC) is a critical parameter for bottom ash reuse, particularly in road construction, as it governs chemical stability and leaching behavior.

The higher TOC levels observed in AT2 compared with AT1 are consistent with findings reported in previous studies [19].

This increase is attributed to limited post-incineration oxidation, retention of organic carbon within the vitreous matrix, and dissolution of mineral phases during soaking, whereas prolonged exposure to heat and oxygen in untreated slags enhances carbon oxidation and lowers TOC. Although elevated TOC may limit certain road applications, post-treatment processes such as curing or controlled carbonation enhance carbon stability and reduce leaching, thereby enabling the use of slags as construction materials [31].

### Mineralogical analysis of bottom ash

Figure 9 shows the percentage distribution of the different materials present in samples AT1 and AT2. Ceramic and ferrous materials increase significantly in AT2 compared to AT1, while the proportion of coal decreases. Glass debris becomes negligible in AT2, indicating effective sorting or removal.

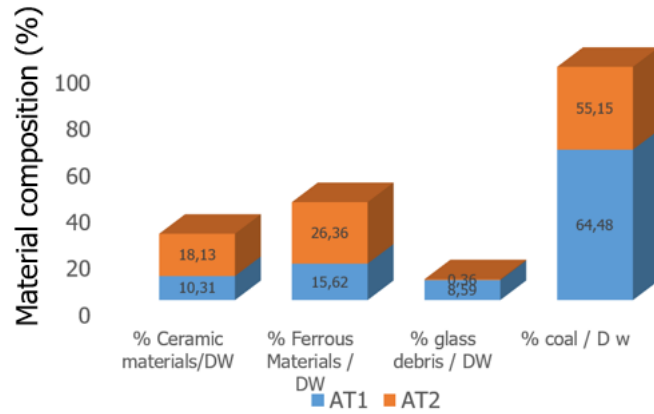


Figure 9. Distribution of recoverable materials in AT1 and AT2 incineration slag samples

### Physical Analysis of Bottom Ash

The physical analysis of bottom ash mainly concerns geotechnical parameters. Four parameters were determined. These include particle size distribution, the density of solid particles, bulk density, and natural moisture content. Figure 10 shows the particle size curves of the two types of bottom ash. The quenched bottom ash (AT2) exhibits a steeper granulometric curve and a narrower particle size distribution compared to the untreated material (AT1), indicating a more homogeneous fragmentation induced by thermal shock. This behavior may indicate improved grading and potentially better suitability for civil engineering applications.

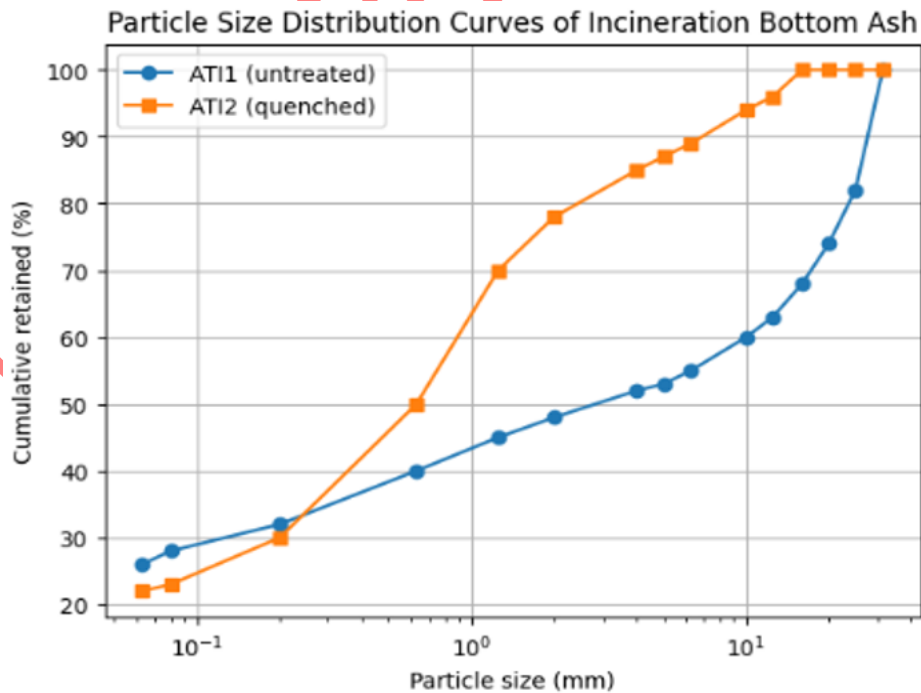


Figure 10. Particle Size Distribution Curves of Incineration Bottom Ash

### ✓ Granulometric and physical properties

The granulometric and physical parameters derived from the particle size distribution curves are summarized in Table 5, including the uniformity coefficient (CU), coefficient of curvature (Cc), fineness modulus (Mf), particle density ( $\rho$ ), bulk density (BD), and moisture content (MC).

Table 5. Physical characteristics of incineration bottom ash

samples	CU	Cc	Mf	P [t/m <sup>3</sup> ]	BD [t/m <sup>3</sup> ]	MC [%]
AT1	434,78	0,097	3,26	2,47	0,86	2
AT2	33,57	1,52	4,51	2,65	0,76	38,9

Dry bottom ash (AT1) exhibits a very high uniformity coefficient (CU = 434.8) combined with a very low coefficient of curvature (Cc = 0.097), indicating an extremely wide and poorly graded particle size distribution. This behavior is characteristic of untreated bottom ash, as reported by [33], and reflects heterogeneous fragmentation resulting from the absence of thermal shock. The fineness modulus (Mf = 3.26) indicates the predominance of coarse fractions, which may be favorable for certain concrete applications, although poor grading can limit compaction. The low bulk density (0.86 t/m<sup>3</sup>) confirms a highly porous structure, consistent with observations reported by [34] for dry bottom ash.

In contrast, quenched bottom ash (AT2) exhibits a lower uniformity coefficient (CU = 33.6) and a coefficient of curvature within the range of well-graded materials (Cc = 1.52). Patel et al. [36] demonstrated that thermal quenching promotes particle fragmentation through the generation of internal thermal stresses. Pierce et al. [35] reported that rapid cooling induces microstructural modifications and crack development resulting from thermal shock. Inkaew et al. [21] observed that water quenching alters particle morphology and contributes to the formation of finer fractions in bottom ash. More recently, Zhang et al. [33] highlighted that cooling conditions significantly influence particle size distribution and material heterogeneity. These findings support the more balanced particle size distribution and improved grading observed for AT2. The higher fineness modulus (Mf = 4.51) confirms the predominance of coarse fractions, while the higher particle density (2.65 t/m<sup>3</sup>) reflects a greater proportion of dense mineral phases and a lower contribution of porous constituents. However, the high moisture content (38.9%) indicates significant saturation, requiring strict control of mixing water during material formulation, as recommended by SETRA–LCPC guidelines.

Overall, wet quenching significantly modifies the granulometric characteristics of bottom ash and promotes a better-graded material. Nevertheless, the associated increase in moisture content must be considered when assessing its suitability for civil engineering applications.

## CONCLUSIONS

This study demonstrates that quenching (AT2) significantly alters the chemical composition, granulometric characteristics, and trace metal stability of industrial incineration bottom ash. Quenched bottom ash shows increased concentrations of basic oxides, notably calcium, aluminum, and phosphorus oxides, along with a more homogeneous distribution of trace metals. These changes may contribute to reduced variability of toxic elements such as cadmium and mercury and could potentially improve the environmental stability of the material.

From a physical perspective, quenching markedly improves particle size distribution and density, with a lower uniformity coefficient (33.6), a curvature coefficient of 1.52, and a higher bulk density of 2.65 t/m<sup>3</sup>, compared with untreated bottom ash, which exhibits a very high uniformity coefficient (434.8), a low curvature coefficient (0.097), and a lower bulk density (2.47 t/m<sup>3</sup>). These changes indicate the formation of a more compact and homogeneous material.

In addition, the higher total organic carbon content observed in quenched ash suggests carbon entrapment within a vitrified matrix, enhancing chemical stability and compatibility with valorization pathways in construction materials. Overall, quenching, combined with complementary treatments such as aging or controlled carbonation, effectively stabilizes bottom ash, optimizes its physicochemical properties, and supports sustainable valorization. Future research should focus on long-term leaching behavior, durability under real service conditions, and life-cycle assessment to enable large-scale application and regulatory acceptance.

### ACKNOWLEDGMENT(S)

The authors gratefully acknowledge the Quality, Safety and Hygiene Manager of RMG Côte d'Ivoire SA for facilitating sample collection.

### Conflicts of Interest

All the authors claim that the manuscript is completely original. The authors also declare no conflict of interest.

### References

- [1] N. N. Nasrudin, N. F. Ariffin, A. M. Hasim, and M. N. S. Zaimi, "A Review: Utilization of Waste Materials in Concrete," *MSF*, vol. 1056, pp. 61–68, Mar. 2022, doi: 10.4028/p-t66fhj.
- [2] H. Hamada, A. Alattar, B. Tayeh, F. Yahaya, and A. Adesina, "Sustainable application of coal bottom ash as fine aggregates in concrete: A comprehensive review," *Case Studies in Construction Materials*, vol. 16, p. e01109, Jun. 2022, doi: 10.1016/j.cscm.2022.e01109.
- [3] K. Chen, Z. Zhang, F. Qu, B. Chen, Z. Tang, and W. Li, "Maximising the use of municipal solid waste incineration bottom ash for sustainable and high-performance cementitious composites," *Developments in the Built Environment*, vol. 23, p. 100717, Oct. 2025, doi: 10.1016/j.dibe.2025.100717.
- [4] H. Jin, L. Cheng, J. Liu, C. Chen, and F. Xing, "Recycling and valorization of municipal solid waste incineration bottom ash via cold-bonded granulation technology – The role of fiber volume and fiber type," *Construction and Building Materials*, vol. 442, p. 137427, Sep. 2024, doi: 10.1016/j.conbuildmat.2024.137427.
- [5] J. Xiao, K. Zhang, T. Ding, Q. Zhang, and X. Xiao, "Fundamental Issues Towards Unified Design Theory of Recycled and Natural Aggregate Concrete Components," *Engineering*, vol. 29, pp. 188–197, Oct. 2023, doi: 10.1016/j.eng.2023.03.017.
- [6] A. P. Bayuseno and W. W. Schmahl, "Understanding the chemical and mineralogical properties of the inorganic portion of MSWI bottom ash," *Waste Management*, vol. 30, no. 8–9, pp. 1509–1520, Aug. 2010, doi: 10.1016/j.wasman.2010.03.010.
- [7] J. R. Minane and R. Vinai, "Bottom Ash: Production, Characterisation, and Potential for Recycling," in *Minerals and Waste*, M. Tribaudino, D. Vollprecht, and A. Pavese, Eds., in Earth and Environmental Sciences Library. , Cham: Springer International Publishing, 2023, pp. 155–212. doi: 10.1007/978-3-031-16135-3\_7.
- [8] Y. Huang, L. Wang, T. Wu, W. Liu, and Q. Tang, "Mechanical properties and heavy metal leaching behaviors of municipal solid waste incineration bottom ash as road

- embankment fillings,” *Journal of Cleaner Production*, vol. 394, p. 136355, Mar. 2023, doi: 10.1016/j.jclepro.2023.136355.
- [9] M. Šyc *et al.*, “Metal recovery from incineration bottom ash: State-of-the-art and recent developments,” *Journal of Hazardous Materials*, vol. 393, p. 122433, Jul. 2020, doi: 10.1016/j.jhazmat.2020.122433.
- [10] H. Vandersloot, “Leaching behaviour of waste and stabilized waste materials; characterization for environmental assessment purposes,” *Waste Management & Research*, vol. 8, no. 3, pp. 215–228, Jun. 1990, doi: 10.1016/0734-242X(90)90065-U.
- [11] J. A. Meima and R. N. J. Comans, “Geochemical Modeling of Weathering Reactions in Municipal Solid Waste Incinerator Bottom Ash,” *Environ. Sci. Technol.*, vol. 31, no. 5, pp. 1269–1276, Apr. 1997, doi: 10.1021/es9603158.
- [12] O. Hammoud, D. Blanc, M. Lupsea-Toader, and C. De Brauer, “Geochemical modeling of the leaching behavior of municipal solid waste bottom ash,” *Environnement, Ingénierie & Développement*, vol. N° 85-EID, p. 7696, Nov. 2021, doi: 10.46298/eid.2021.7696.
- [13] Y. He and M. Kasina, “The Sequential Extraction of Municipal Solid Waste Incineration Bottom Ash: Heavy Metals Mobility and Sustainable Application of Ashes,” *Sustainability*, vol. 15, no. 19, p. 14638, Oct. 2023, doi: 10.3390/su151914638.
- [14] M. Izquierdo and X. Querol, “Leaching behaviour of elements from coal combustion fly ash: An overview,” *International Journal of Coal Geology*, vol. 94, pp. 54–66, May 2012, doi: 10.1016/j.coal.2011.10.006.
- [15] F.-G. Simon and P. Scholz, “Assessment of the Long-Term Leaching Behavior of Incineration Bottom Ash: A Study of Two Waste Incinerators in Germany,” *Applied Sciences*, vol. 13, no. 24, p. 13228, Dec. 2023, doi: 10.3390/app132413228.
- [16] J. J. Dijkstra, A. Van Zomeren, J. C. L. Meeussen, and R. N. J. Comans, “Effect of Accelerated Aging of MSWI Bottom Ash on the Leaching Mechanisms of Copper and Molybdenum,” *Environ. Sci. Technol.*, vol. 40, no. 14, pp. 4481–4487, Jul. 2006, doi: 10.1021/es052214s.
- [17] H. Kubota, K. Shigeizumi, T. Fujikawa, C. Koga, and K. Sato, “An Accelerated, On-Site Bottom Ash Aging and Washing Treatment and Its Effect for Long-Term Leaching,” *Waste Biomass Valor*, vol. 11, no. 12, pp. 7067–7077, Dec. 2020, doi: 10.1007/s12649-020-01136-9.
- [18] L. Lombardi and E. A. Carnevale, “Bottom Ash Treatment at the Site of Producing Plant for Reutilization,” *Waste Biomass Valor*, vol. 7, no. 4, pp. 965–974, Aug. 2016, doi: 10.1007/s12649-016-9551-z.
- [19] A. Glauser, L. S. Morf, G. Weibel, and U. Eggenberger, “Ten-years monitoring of MSWI bottom ashes with focus on TOC development and leaching behaviour,” *Waste Management*, vol. 117, pp. 104–113, Nov. 2020, doi: 10.1016/j.wasman.2020.07.038.
- [20] J. Xiao, Z. Lv, Z. Duan, and C. Zhang, “Pore structure characteristics, modulation and its effect on concrete properties: A review,” *Construction and Building Materials*, vol. 397, p. 132430, Sep. 2023, doi: 10.1016/j.conbuildmat.2023.132430.
- [21] K. Inkaew, A. Saffarzadeh, and T. Shimaoka, “Modeling the formation of the quench product in municipal solid waste incineration (MSWI) bottom ash,” *Waste Management*, vol. 52, pp. 159–168, Jun. 2016, doi: 10.1016/j.wasman.2016.03.019.
- [22] I. S. Samaka, A. Al-Janabi, M. Abdulredha, A. Alkandari, M. Abdellatif, and D. Yeboah, “Reusing of furnace bottom ash as an adsorbent for phosphate removal from water,” *IOP Conf. Ser.: Mater. Sci. Eng.*, vol. 1058, no. 1, p. 012006, Feb. 2021, doi: 10.1088/1757-899X/1058/1/012006.
- [23] C.-L. Lin, Z.-Y. Chen, and Z.-S. Liu, “Transforming waste into value: High-performance hollow fiber adsorbents from municipal solid waste incinerator bottom ash,” *Waste Management*, vol. 204, p. 114956, Aug. 2025, doi: 10.1016/j.wasman.2025.114956.

- [24] Y. Zhao, W. Li, J. Wang, and Z. Hu, "A Sustainable Development Strategy for Municipal Solid Waste Incineration Bottom Ash: Adsorption Performance and Mechanism in Removing Heavy Metals from Water," *Sustainability*, vol. 17, no. 8, p. 3466, Apr. 2025, doi: 10.3390/su17083466.
- [25] H. Li, Z. Yin, L. Deng, S. Wang, Z. Fu, and Y. Ma, "Effect of SiO<sub>2</sub>/Al<sub>2</sub>O<sub>3</sub> ratio on the structure and electrical properties of MgO–Al<sub>2</sub>O<sub>3</sub>–SiO<sub>2</sub> glass-ceramics doped with TiO<sub>2</sub>," *Materials Chemistry and Physics*, vol. 256, p. 123653, Dec. 2020, doi: 10.1016/j.matchemphys.2020.123653.
- [26] S. Zhang *et al.*, "Effects of soil amendments on soil acidity and crop yields in acidic soils: A world-wide meta-analysis," *Journal of Environmental Management*, vol. 345, p. 118531, Nov. 2023, doi: 10.1016/j.jenvman.2023.118531.
- [27] M. Muhajir, P. Puspitasari, and J. A. Razak, "Synthesis and Applications of Hematite  $\alpha$ -Fe<sub>2</sub>O<sub>3</sub>: a Review," *JMEST*, vol. 3, no. 2, pp. 51–58, Nov. 2019, doi: 10.17977/um016v3i22019p051.
- [28] J. M. Cases and F. Thomas, Eds., *Proceedings of the International Congress on Waste Solidification-Stabilisation Processes: 28 November-1st December 1995, Nancy, France = Actes du Congrès international sur les procédés de solidification et de stabilisation des déchets / J.M. Cases and F. Thomas, editors*. Grenoble: Société alpine de publications, 1997.
- [29] Y. Song *et al.*, "Effect of pre-aging on the microstructure and properties evolution of cold-rolled Cu-Ni-Co-Si during final aging," *Materials Characterization*, vol. 223, p. 114957, May 2025, doi: 10.1016/j.matchar.2025.114957.
- [30] S. Durecu, Venditti, D, D. Goy, Thauron, J, and Berthelin, J, "Stabilization by the Tredi-Ash process for slags issued by industrial waste incineration plants," presented at the International congress on waste solidification-stabilisation processes, France, Dec. 1997, pp. 103–106.
- [31] W. Jiang, Y. Huang, and A. Sha, "A review of eco-friendly functional road materials," *Construction and Building Materials*, vol. 191, pp. 1082–1092, Dec. 2018, doi: 10.1016/j.conbuildmat.2018.10.082.
- [32] S. M. Davarpanah, S. Narimani, M. Sharghi, and B. Vásárhelyi, "Introducing Coefficients of Curvature (Cc) and Uniformity (Cu) Based on RQD for Rock Mass Characterization," *RML*, vol. 2, no. 1, pp. 76–78, Mar. 2025, doi: 10.70425/rml.202501.10.
- [33] H. Zhang, C. Wang, Z. Chen, Q. Kang, X. Xu, and T. Gao, "Performance Comparison of Different Particle Size Distribution Models in the Prediction of Soil Particle Size Characteristics," *Land*, vol. 11, no. 11, p. 2068, Nov. 2022, doi: 10.3390/land11112068.
- [34] L. P. Lossius, B. Spencer, and H. A. Øye, "Bulk Density - Overview of ASTM and ISO Methods With Examples of Between Laboratory Comparisons," in *Light Metals 2011*, S. J. Lindsay, Ed., Cham: Springer International Publishing, 2011, pp. 941–946. doi: 10.1007/978-3-319-48160-9\_161.
- [35] D. T. Pierce *et al.*, "Microstructural evolution during quenching and partitioning of 0.2C-1.5Mn-1.3Si steels with Cr or Ni additions," *Acta Materialia*, vol. 151, pp. 454–469, Jun. 2018, doi: 10.1016/j.actamat.2018.03.007.